UNIVERSITY OF CALIFORNIA, SAN DIEGO

Innate Immune Response to Rotavirus Infection is Differentially Modulated by MAVS and TLR3 Signaling

A Thesis submitted in partial satisfaction of the
requirements for the degree Master of Science

in

Biology

by

Michael Raymond Wang

Committee in charge:

Professor Martin F. Kagnoff, Chair
Professor Michael I. David, Co-Chair
Professor Elina I. Zuniga

2012

The Thesis of Michael Raymond Wang is approved and it is acceptable in quality and form for publication on microfilm and electronically:

_____

_____

Co-Chair

_____

Chair

University of California, San Diego

2012

TABLE OF CONTENTS

LIST OF FIGURES

ABSTRACT OF THE THESIS

Innate Immune Response to Rotavirus Infection is Differentially Modulated by MAVS and TLR3 Signaling

by

Michael Raymond Wang

Master of Science in Biology

University of California, San Diego, 2012

Professor Martin F. Kagnoff, Chair

Mammalian cells can detect the presence of viral double-stranded RNA (dsRNA) through extracellular and intracellular pathogen recognition receptors (PRRs). Toll-like receptor 3 (TLR3) can be localized on the endosomal membrane of cells and detects endocytosed dsRNA (extracellular). Conversely, RIG-I-like receptors (RLRs), which include retinoic acid inducible gene I (RIG-I) and melanoma differentiation-associated protein 5 (Mda-5) receptors detect dsRNA in the cytoplasm (intracellular). Most IEC types that have been used to study rotavirus infection lack robust TLR3 signaling. Here, via analysis of type I interferon (IFN) induction and apoptosis, the HCT-116 cell line was identified to harbor both TLR3 and RIG/Mda-5 dsRNA signaling pathways. This cell type may be useful for future *in vitro* studies of the role of these extracellular and intracellular signaling pathways in

rotavirus infections. Through a series of experiments using the SA11-4F and SA11-5S strains of rotavirus, it was determined that SA11-4F exerts a suppressive effect on IFN response in HCT-116 cells, likely through an inhibitory effect on IFN regulatory factor 3 (IRF-3) caused by nonstructural protein 1 (NSP1), as has been shown by others. It was also observed that MAVS is required for maximal IFN-β induction in HCT-116 cells following rotavirus infection. Surprisingly, it was determined that TLR3 stimulation exhibits a negative regulatory effect on mitochondrial antiviral signaling protein (MAVS, also known as IPS-1 or Cardif), a mitochondrial surface protein that serves as a common adaptor to RIG-I-like receptors (RLRs). IFN-β induction increased in the absence of TLR3, and this strengthened innate immune response exhibits a biologically relevant reduction in viral replication. These results observed in HCT-116 cells suggest that TLR3 may up-regulate apoptosis following viral infection, and down-regulate MAVS levels and IFN-β production.

INTRODUCTION

The Public Health Relevance of Rotaviruses

For years, rotavirus infection has ranked consistently as one of the most widespread human infectious diseases. Today, an estimated >500,000 lives are claimed worldwide each year as a result of rotavirus-induced gastroenteritis (Ramig, R. F. 2004). The total death toll is currently estimated to be between 3-5 million, and the highest number of infections is observed among children under 5 years of age (Wilhelmi, *et al*., 2003). Rotavirus-induced gastroenteritis can be found in diverse populations and is endemic to many parts of the world, but is especially prevalent among young children under two years of age with the incidence of illness peaking at weaning age (Bartlett, *et al*., 1987). The geographical origins of rotavirus strains are still unclear today, however, the viruses are known to have originated within a temperate region of the globe (Wolfe, *et al*., 2007). The introduction of rotaviruses to humans, and therein the existence of rotavirus-induced human illnesses, likely did not occur until the development of agriculture and the domestication of livestock within ancient human civilizations (Wolfe, *et al*., 2007).

Rotavirus Phylogenic Background

Rotaviruses are grouped into the *Reoviridae* family of viruses and are the pathogenic species primarily responsible for eliciting acute diarrhea and severe gastroenteritis in children, as well as in some animals (Estes, *et al.*, 1983; Kapikian & Chanock, 1985). Although not limited to small intestinal infection, rotavirus

primarily infiltrates small intestinal epithelial cells, causing diminished efficiency in villus absorption of disaccharides, ions, and water by enterocytes (Ramig, R. F., 2004). The most severe damage can often be found in the proximal region of the small intestinal tract (Rollo, *et al*., 1999; Ciarlet, *et al*., 2001). There are six characterized serogroups of rotaviruses (A, B, C, D, E and F); groups A through C exist among both human and animal populations, while groups D through F are found exclusively in animals (Estes & Cohen, 1989).

The Structural Components of Rotaviruses

The structural morphology of rotaviruses is complex. They contain outer and inner spherical shells that protect a core protein comprising of an 11-segmented viral double-stranded RNA (dsRNA) genome (Estes *et al*., 1983). The viral genome is housed within a triple-layered protein capsid coat, and synthesizes six structural viral proteins, as well as six non-structural viral proteins that serve distinct functions. These dsRNA segments vary between 667 to 3,302 base pairs long, with the complete rotavirus genome totaling about 18,500 base pairs (Rixon, *et al*., 1984). Rotavirus depends on an RNA-dependent RNA polymerase to achieve transcription of mRNA from its dsRNA segments (Cohen, 1977).

Rotavirus particles are relatively large in size, measuring approximately 75 nm in diameter (Estes & Cohen, 1989). While the rotavirus structural proteins (VP1 to VP4, VP6 and VP7) are responsible for maintaining the integrity of the viral capsid, the nonstructural proteins (NSPs) have a diverse range of functions. The

roles of nonstructural proteins are still being elucidated, but these proteins may be involved in RNA binding, gene replication, synthesis and packaging of viral RNA, and cellular translocation (J. T. Patton, 1995). Although they are contained within the virion, they are expressed within an infected host (Bagchi, *et al.*, 2010).

Out of the 6 known rotavirus NSPs (NSP1 to NSP6), non-structural protein 1 (NSP1) is of particular interest. NSP1 is the only viral protein encoded by gene 5 of the viral genome. It is the least conserved NSP within different strains of rotavirus, and also does not appear to be essential for viral replication and survival within the host cell, which was observed with rotavirus strains encoding truncated versions of the protein (Mitchell & Both, 1990; Taniguchi, K., *et al*., 1996). Moreover, NSP1 has been observed to harbor roles in regulating viral gene expression by way of two IFN inhibitory mechanisms, both mediated through proteasome-dependent degradation (Bagchi, *et al*., 2010; Chattopadhyay, *et al*., 2010). NSP1 has been shown to induce degradation of IFN regulatory factors (IRFs) such as IRF-3, IRF-5 and IRF-7 to block IFN gene activation, and also degrades β-TrCP to disrupt NFκB signaling (Barro & Patton, 2005; Barro & Patton, 2007; Graff, *et al*., 2002; Graff, *et al*., 2009). Recent studies revealed that NSP1 may also disrupt RIG-I signaling in a proteasome-independent manner (Qin, *et al*., 2011).

Mammalian Host Innate Recognition of Rotavirus Infection

Many advances were made in understanding viral pathogenesis and host responses to viral infections in the past decade. During viral or bacterial infection in

mammalian cells, membrane-bound or cytoplasmic pattern recognition receptors (PRRs) recognize specific pathogen associated molecular patterns (PAMPs) to activate a host innate immune response (Akira, S., 2001; Takeda, K., *et al*, 2003). There are specific PRR families that recognize viral double-stranded RNA (dsRNA), namely RIG-I-like receptors (RLRs) and Toll-like receptors (TLRs). Retinoic inducible gene I (RIG-I), and melanoma differentiation-associated gene 5 (Mda-5), are two cytoplasmic RIG-I-like RNA helicases that have been shown to induce an innate immune response (Kawai, T., *et al*., 2005; Broquet, *et al*., 2011). It has been suggested that although RIG-I and Mda-5 both detect viral dsRNA, they may recognize dsRNA that vary in size or originate from different viruses (Kato, et al., 2006). Moreover, it has been shown that RLRs are required to induce a type I IFN response *in vitro* in IECs (Kato, et al., 2006; Broquet, *et al*., 2011). Laboratory of genetics and physiology 2 (LGP2) is the third known RLR, but does not rely on the same adaptor protein (MAVS) as RIG-I and Mda-5 for downstream signaling (Hirata, *et al*., 2007). Since LGP2 is also a cytosolic receptor, it competes with RIG-I and Mda-5 as a cytoplasmic dsRNA detector, and may thus act as a negative regulator of MAVS signaling (Rothenfusser, *et al*., 2005; Saito, *et al*., 2007).

Following viral-penetration into the host cytoplasm, cytosolic RLRs are able to recognize and bind to intracellular dsRNA to elicit an innate antiviral immune response (Yoneyama, *et al.*, 2004). Type I IFN expression and signaling is induced, and causes the transient activation of IFN-stimulated response elements (ISREs) (Taniguchi, T. & Takaoka, 2002). This activation effect in IECs can be mimicked *in*

vitro by introducing synthetic dsRNA in the form of polyinosinic polycytidylic acid [poly(I:C)] into the IEC cytoplasm, which likewise results in an increase in type I IFN production via activation of RLRs (Yoneyama, et al., 2005). RLRs activate the mitochondrial antiviral signaling protein (MAVS), a mitochondrial membrane-bound adaptor protein that is also alternatively referred to in literature as IFN-β promoter stimulator (IPS-1), Cardif, or VISA (Seth, R. B., *et al*., 2005; Kawai, T., *et al.*, 2005; Meylan, E., *et al*., 2005; Xu, L. G., *et al*., 2005). Upon binding to dsRNA, RLRs signal to MAVS, which then leads to the activation of IFN regulatory factor 3 (IRF-3), a key transcription factor involved in the regulation of ISREs.

TLRs, on the other hand, have the ability to discriminate a wide variety of pathogens. TLR1, TLR2, TLR4 and TLR6 detect lipid ligands, while TLR5 is specialized in recognizing flagellin, and TLR3, TLR7, TLR8 and TLR9 are able to detect foreign nucleic acids (Kaisho & Akira, 2005). Five of the identified Toll-like receptors, TLR1 to TLR4, and TLR9, are known to be expressed in small intestinal epithelial cells (IECs) (Otte, et al., 2004). TLRs sense specific PAMPs via a leucine-rich repeat region binding domain. The leucine-rich repeat region for TLR3 recognizes dsRNA and initiates TLR3's interaction with the TRIF adaptor protein, subsequently leading to IRF-3-phosphorylation (Akira & Takeda, 2004). The downstream signaling following these pattern recognitions leads to the production of type I IFNs. TLR3 relies on a Myd88-independent pathway, however most of the other Toll-like receptors signal through a Myd88-dependent pathway, and TLR4 is

unique in the sense that it can signal through both Myd88 dependent and independent pathways (Yamamoto, *et al*., 2003).

Much like its role as a dsRNA ligand for RIG-I and Mda-5 signaling, poly(I:C) can also be used as a synthetic ligand for activating TLR3-signaling (Alexopoulou, *et al*., 2001; Yamamoto, *et al*., 2003). TLR3 is expressed in both IECs of the small intestine, as well as in IECs of the colon (Cario & Podolsky, 2000). TLR3 exists on endosomal membranes and has the ability to recognize extracellular viral dsRNA that has been endocytosed from the plasma membrane (Akira, S., 2001; Alexopoulou, L., *et al*., 2001). Upon its activation, TLR3 can lead to the activation of the pathways for NF-κB and mitogen-activated protein (MAP) kinases, as well as in the activation of type I IFN (Alexopoulou, *et al*., 2001).

Upon viral infection, the host cells respond by increasing synthesis of type I IFNs, which include IFN-α and IFN-β. Increased type I IFN production further triggers the expression of anti-viral genes within infected cells, and alerts neighboring cells, in a positive feedback fashion. To ensure their own viability and livelihood upon infecting their hosts, many viruses have developed mechanisms for disrupting the host's innate immunological defense system. An evolutionarily common approach for doing so involves inhibition of type I IFN production.

Mammalian Innate Immune Response to Rotavirus Infection

Previous research suggested that NSP1 antagonizes type I IFN production in infected host cells by inhibiting IRF-3 activity (Barro & Patton, 2005; Barro &

Patton, 2007; Bagchi, *et al*., 2010). During IRF-3 activation, phosphorylation occurs at serine-residues mediated by TANK-binding kinase 1 (TBK1) and IKKε, which are both kinases from the IκB kinase family (Fitzgerald, *et al*., 2003; Sharma, *et al*., 2003). After phosphorylation, activated-IRF-3 is translocated into the nucleus where it binds to the IFN-β promoter for inducing IFN gene activity (Yoneyama, *et al.*, 1998; Taniguchi, T. & Takaoka, 2002). IRF-7 has also been characterized as being an important transcription factor for type I IFN expression. Much like IRF-3, IRF-7 undergoes phosphorylation and subsequent translocation into the nucleus in the event of viral infection to act as a transcription factor for gene regulation (Sato, *et al*., 1998). Constitutively expressed IRF-3 may be primarily responsible for eliciting an initial IFN response to viral infection, whereas IRF-7 may play a greater role in positively regulating IFN-α and IFN-β production later on in the innate immune response (Sato, et al., 2000). IRF-3 inhibition by NSP1 would therefore not only interfere with the transcription factor's dimerization and translocation into the nucleus to allow for IFN gene activity, but would also prevent the robust IFN response that it typically induces along with IRF-7.

There are many different strains of rotaviruses; however, in this study, I focused on two simian rotavirus strains, termed SA11-4F and SA11-5S. The only difference between these two strains of simian rotaviruses is in the nature of their encoded NSP1. The NSP1 of both strains is encoded by gene 5 of the rotaviral genome, with SA11-4F possessing a wild-type NSP1, and SA11-5S expressing a C-

terminal truncated version of NSP1 protein lacking 17 amino acids (Patton, *et al*., 2001; Barro and Patton, 2005).

Apoptosis in Mammalian Cells as a Mechanistic Response to Rotavirus Infection

Apoptosis is a common innate immune response to cellular infection, and serves the purpose of ridding the host of genetically damaged or viral-infected cells (Chawla-Sarkar, *et al*., 2003). In the case of viral infection, increased type I IFN levels may lead to activation of caspase-8, and subsequently caspase-3 signaling to induce apoptosis (Chawla-Sarkar, *et al*., 2003). One hallmark of this self-destructive process common to mammalian cells is poly(ADP-ribose) polymerase (PARP) proteolytic cleavage (Lazebnik, *et al*., 1994), which is achieved by activation of caspase pathways (Salvesen & Dixit, 1997).

Specific Aims for this Master's project

Previously, the Kagnoff Lab demonstrated that the RIG-I/Mda-5/MAVS pathway is activated by simian rotavirus infection in HT-29 and HCA-7 human intestinal epithelial cell lines (Broquet*, et al*., 2011). However, a recent study showed that the TLR3/TRIF pathway may also be important in protection against a murine rotavirus strain (Pott, *et al*., 2012). To date, most of the cell lines that have been studied do not respond strongly to viral dsRNA via TLR3-signaling. I therefore wanted to find and utilize a cell line that could exhibit a strong TLR3-dependent response, and to characterize the innate immune responses to rotavirus infection in

these cells by examining IFN-β induction and cellular apoptosis. A study conducted by Taura, *et al*. showed that HCT-116 human colonic epithelial cell line strongly expresses TLR3 in a p53-dependent manner and responds to extracellular poly(I:C) stimulation (Taura, *et al*., 2008). The tumor suppressor protein binds to the p53-binding domain in the TLR3 promoter, and subsequently enhances the expression of TLR3, suggesting the HCT-116 cell line's potential reliance on TLR3-signaling.

RESULTS

Type I Interferon induction in poly(I:C)-treated HT-29 and HCT-116 Cells

To compare the innate immune response to dsRNA among different intestinal epithelial cell lines, I conducted a series of *in vitro* experiments using two established human intestinal epithelial cell lines, HCT-116 cells and HT-29 cells, the latter of which was used in previous studies conducted by the Kagnoff Laboratory (Broquet, *et al*., 2011). I treated the respective cell lines with a low molecular weight (LMW) poly(I:C), a synthetic dsRNA with an average size of 300 bp, to determine IFN-β induction levels in response to dsRNA. Poly(I:C) was either added to cell culture media, or transfected into cells using a transfection reagent, and 2 biological replicates were performed for each cell type. When poly(I:C) was placed into cell culture media, HCT-116 cells exhibited a 125-fold increase in IFN-β induction following LMW poly(I:C) treatment, while in HT-29 cells, IFN-β was increased by only 13-fold after LMW poly(I:C) treatment, respectively (**Fig. 1A**). LMW poly(I:C) transfection yielded a nearly 3-fold greater level of IFN-β expression in HT-29 than in HCT-116 cells (**Fig. 1B**) Therefore in sum, HT-29 responded weakly to poly(I:C) present in the media, but produced a robust IFN-induction when poly(I:C) was transfected. HCT-116 cells exhibited comparable levels of IFN-β induction when dsRNA was transfected into cells, whereas they demonstrated much higher levels of IFN-β induction in media-treated (extracellular dsRNA) conditions compared to HT-29 cells. These data confirm that HCT-116 cells respond to both extracellular and intracellular dsRNA stimulation. To rule out residual effects of the

transfection reagent used, mock transfections were conducted without poly(I:C) and resulted in no IFN-inductive effects. HCT-116 cells are therefore a promising cell line to study viral pathogenesis, for which both TLR3/TRIF and RIG-I/Mda-5/MAVS detection of dsRNA has been observed (Zhou, *et al*., 2007; Broquet, *et al*., 2011). Its dependency on TLR3/TRIF signaling is useful for understanding whether detection of extracellular dsRNA would have any impact on rotavirus replication within the mammalian host, and whether this detection could enhance the host's ability to clear virus upon infection.

Type I Interferon induction in poly(I:C)-treated and gene-silenced HCT-116 cells

In an effort to further characterize the signaling pathways involved in the innate anti-viral response to dsRNA in HCT-116 cells, and to confirm the requirement of TLR3 for extracellular dsRNA sensing, TLR3 and MAVS gene expression were knocked down using siRNA. Poly(I:C) was mixed with cell culture media or transfected into host cells, following pretreatment of the cells with siRNA (**Fig. 2**). TLR3-silencing suppressed IFN gene activation by 3-fold in response to poly(I:C) in media. On the other hand, knockdown of MAVS generated a nearly 6-fold higher level in IFN gene induction following dsRNA in the media. This demonstrates the role of TLR3 in innate signaling for extracellular dsRNA detection in HCT-116 cells that is MAVS independent (**Fig. 2A**). Cells that were exposed to intracellular dsRNA via transfection exhibited the opposite trend. MAVS-silenced HCT-116 cells showed a 5-fold lower level in IFN-β response compared to cells

treated with control-siRNA (**Fig. 2B**). This indicates that intracellular detection of dsRNA depends on a RIG-I/Mda-5/MAVS pathway signaling.

PARP cleavage in poly(I:C)-treated HT-29 and HCT-116 cells

IEC apoptosis induced by dsRNA was assessed by detection of poly ADP-ribose polymerase (PARP) cleavage via immunoblotting in HCT-116 and HT-29 cells following poly(I:C)-treatment (**Fig. 3**). Once again, cells were exposed to dsRNA via both extracellular or intracellular delivery in order to observe cellular responses to different localization of dsRNA. Although cleaved PARP bands for HT-29 extract samples were very faint, PARP-cleavage was observed for HT-29 cells transfected (intracellular) with poly(I:C) (**Fig. 3, Lane 3**), while samples treated with poly(I:C) culture media (extracellular) exhibited no observable cleavage (**Fig. 3, Lane 2**). Poly(I:C)-treated HCT-116 cells, on the other hand, yielded similar levels of PARP cleavage for both routes of poly(I:C) delivery (**Fig. 3, Lane 5 & 6**), consistent with the hypothesized dual-dependency of extracellular TLR3 and intracellular RLR signaling in this cell line. These trends in apoptosis as assessed by PARP cleavage were similar to the type I IFN induction trends shown in **figure 1**.

Type I Interferon induction in rotavirus-infected HCT-116 cells

In order to better simulate *in vivo* viral pathogenesis in an *in vitro* system, I compared the effect of rotavirus infection on IFN-β induction levels in HCT-116 cells with the effect of poly(I:C) treatments in HCT-116 cells (**Figs. 1 & 2**). To accomplish

this, SA11-4F and SA11-5S rotavirus strains were used to infect TLR3 and MAVS gene-silenced HCT-116 cells. In the absence of siRNA, IFN-β gene fold induction levels were significantly higher in SA11-5S-infected cells compared to in SA11-4F-infected cells (**Fig. 4**). This was consistent with the previously reported inhibitory effect by the SA11-4F NSP1 on type I IFN production in the Caco-2 colon epithelial cell line (Barro & Patton, 2007). MAVS-silenced cells had noticeably lower levels of IFN-β expression following SA11-4F- and SA11-5S-infection than control- and TLR3-siRNA treated samples (**Figs. 5A & 5B**). Consistent with previous observations for poly(I:C)-treatment, TLR3-silencing enhanced IFN-β induction following SA11-4F- and SA11-5S-infection (**Figs. 5A & 5B**).

SA11-4F NSP1 prevents IRF-3-phosphorylation in HCT-116 cells

In a 2005 study conducted by M. Barro and J. T. Patton, NSP1 was shown to degrade IRF-3, resulting in a drop in IRF-3 dimerization and nuclear translocation levels, as well as an overall decrease in type I IFN production (Barro & Patton, 2005). To explore whether NSP1 could be responsible for the differential effects of IFN-β induction observed in **figure 4**, I looked for IRF-3-phosphorylation levels in rotavirus-infected and poly(I:C)-treated HCT-116 sample protein extracts, as well as for signs of IRF-3 degradation or inhibition via immunoblot analysis. Through several experiments, I observed IRF-3-phosphorylation in SA11-5S rotavirus-infected intestinal epithelial cells (**Fig. 6, Lanes 5-8**), but interestingly, no IRF-3-phosphorylation in SA11-4F rotavirus-infected cells (**Fig. 6, Lanes 1-4**). After re-

probing the nitrocellulose membranes with total-IRF-3 antibody, IRF-3 levels were similar for SA11-4F- and SA11-5S-treated samples.

The similarity in total-IRF-3 levels observed between SA11-4F- and SA11-5S-infected HCT-116 cells (**Fig. 6**), suggests that SA11-4F NSP1 may selectively degrade phosphorylated-IRF-3. The other possibility that explains similar total-IRF-3 levels between the two strains is that SA11-4F NSP1 could prevent IRF-3 phosphorylation in another manner. While total-IRF-3 levels were reduced following control-siRNA and MAVS-siRNA treatment (**Fig. 6, Lanes 6 & 8**), IRF-3 phosphorylation still occurred in the control-siRNA-treated sample (**Fig. 6, Lane 6**). However, I observed a significant reduction in the phosphorylation levels of IRF-3 protein in MAVS-silenced SA11-5S-infected HCT-116 cells (**Fig. 6, Lane 8**), compared to SA11-5S-infected HCT-116 cells that had been transfected with no siRNA, control-siRNA, or TLR3-siRNA (**Fig. 6, Lanes 5-7**), supporting a role for MAVS in activation of IRF-3-dependent IFN-signaling by SA11-5S rotavirus.

Knockdown of TLR3 prevents reduction in MAVS, following SA11-5S Infection

When TLR3 was silenced, HCT-116 cells exhibited increased levels of IFN-β induction compared to cells transfected with control-siRNA, possibly suggesting a suppressive activity of TLR3 on MAVS-dependent innate immune signaling (**Figures 5B & 5C**). To test this hypothesis, I utilized a rabbit anti-MAVS antibody to analyze differences in MAVS protein-levels in rotavirus-infected HCT-116 cells. Anti-MAVS probing revealed noticeably reduced levels of MAVS protein in SA11-5S-infected

HCT-116 cells (**Fig. 7A, Lanes 4 & 8**), but not in poly(I:C)-treated or SA11-4F-infected cells in control conditions (**Fig. 7A, Lanes 2-3 & 6-7**). Conversely, in the absence of TLR3, SA11-5S-infected cells did not yield a reduction in MAVS (**Fig. 7B, Lane 4**). This suggests that the presence of TLR3 during SA11-5S-infection may somehow reduce levels of MAVS, therefore possibly explaining the IFN induction trends observed after TLR3 silencing in SA11-5S-infected cells (**Figs. 5B & 5C**).

PARP cleavage in rotavirus-infected HCT-116 cells

The increased IFN-β induction seen following TLR3 knockdown may be explained by a TLR3-dependent activation of apoptosis in HCT-116 cells following SA11-5S infection, which would result in the decrease in MAVS protein levels that we observed. I began analyzing this possibility by observing PARP-cleavage in SA11-4F- and SA11-5S-infected, gene-silenced HCT-116 cells. A significant difference in PARP-cleavage was not observed when comparing the differences in PARP-cleavage between the control samples and the SA11-4F- and SA11-5S-infected cells (**Fig. 8**). It is likely that given the HCT-116 cells were harvested 36-hours post-infection, the samples had already yielded significant levels of cell death as observed in mock-treated (no siRNA) wells (**Fig. 8A, Lane 1**). This inherent cell death may have masked any differences in levels of PARP-cleavage caused by NSP1 anti-apoptotic effects. However, under all treatment conditions, which included no treatment, poly(I:C)-treatment, SA11-4F-infection, and SA11-5S-infection, PARP-cleavage was consistently higher in HCT-116 cells pre-treated with control-siRNA

and MAVS-siRNA (**Fig. 8A, Lanes 2 & 4**), while PARP-cleavage was consistently reduced in TLR3-silenced HCT-116 cells (**Fig. 8A, Lane 3**).

SA11-5S rotavirus titers for HCT-116 samples

To confirm that the differences in IFN-β induction observed following SA11-5S infection were biologically relevant, supernatant from infected HCT-116 cells was collected in order to determine the viral burden in the various treatment conditions. We focused on determining viral titers for SA11-5S rotavirus because it resulted in overall higher levels of type I IFN induction in HCT-116 cells than in SA11-4F rotavirus. HCT-116 cells were infected with a SA11-5S viral stock concentration of 3×10^8 virus particles/mL. A plaque assay on MA104 cells revealed that viral supernatant collected from TLR3-silenced rotavirus-infected HCT-116 cells yielded 1.55×10^6 PFU/mL, which is approximately half the amount of plaque-forming units (PFU) compared to that of viral supernatant collected from samples with no siRNA at 3.35×10^6 PFU/mL, siRNA-Control at 3.0×10^6 PFU/mL, and siRNA-MAVS at 3.0×10^6 PFU/mL respectively (**Fig. 9**). This correlates to the type I IFN induction results presented in **figure 5**. TLR3-silenced HCT-116 cells consistently yielded the highest levels of IFN-β induction, which suggests that the lower PFU observed here for TLR3-silenced samples may be due to a type I IFN-production difference. Conversely, MAVS-silenced samples did not result in a fewer number of plaques. This observation corresponds to the suppressed IFN-induction trends observed for MAVS-deficient samples in **figure 5**.

Figure 1. IFN-β induction in poly(I:C)-treated HT-29 and HCT-116 cells.
Low molecular weight (LMW) poly(I:C) was used as synthetic dsRNA for activating innate signaling pathways in HCT-116 cells. dsRNA treatment was conducted by mixing poly(I:C) with cell culture media (10μg/mL), or by transfecting into cells (2μg). RNA samples were harvested 6 hours post-treatment, and IFN-β gene induction levels were compared against baseline GAPDH gene expression levels by quantitative real-time PCR analysis. Values are mean ± s. d. from 3 experimental replicates per treatment.

(A) IFN-β gene induction in HT-29 and HCT-116 cells, treated with LMW poly(I:C).

(B) IFN-β gene induction in HT-29 and HCT-116 cells, transfected with LMW poly(I:C).

(A)

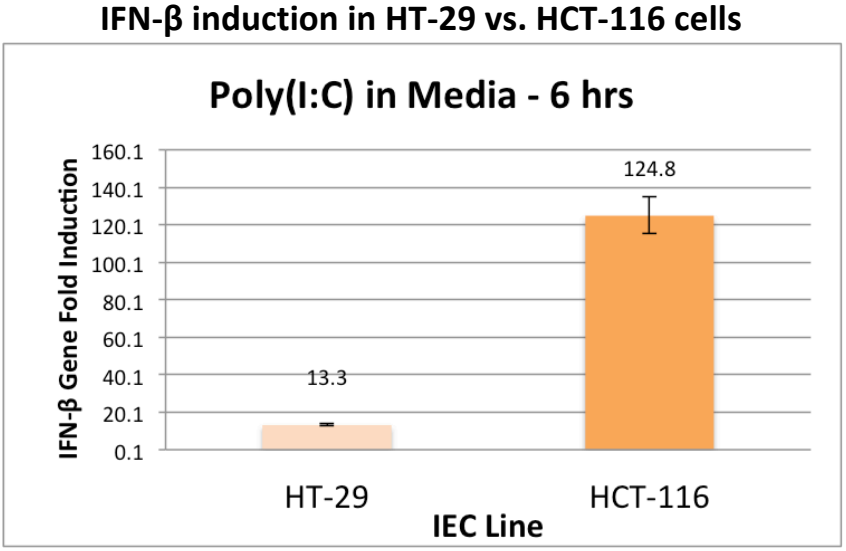
IFN-β induction in HT-29 vs. HCT-116 cells
Poly(I:C) in Media - 6 hrs
IFN-β Gene Fold Induction
160.1
140.1
120.1
100.1
80.1
60.1
40.1
20.1
0.1
124.8
13.3
HT-29
HCT-116
IEC Line

(B)

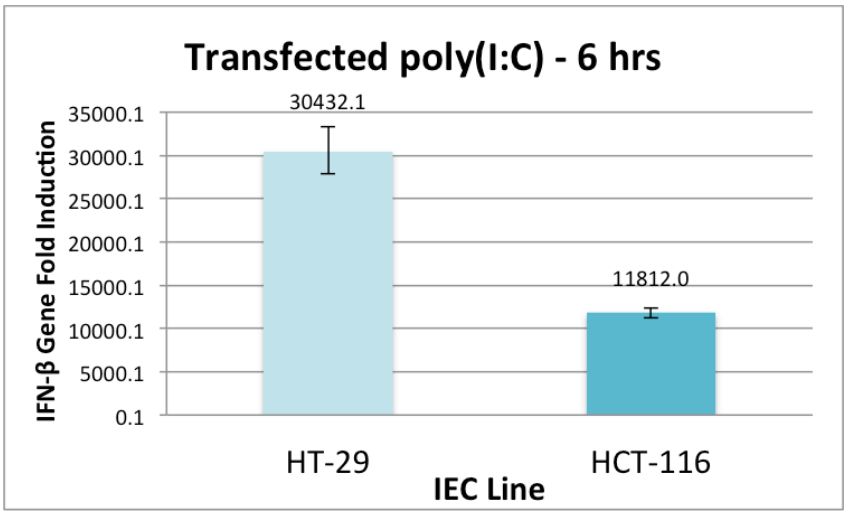
IFN-β induction in HT-29 vs. HCT-116 cells
Transfected poly(I:C) - 6 hrs
IFN-β Gene Fold Induction
35000.1
30000.1
25000.1
20000.1
15000.1
10000.1
5000.1
0.1
30432.1
11812.0
HT-29
HCT-116
IEC Line

Figure 2. IFN-β gene induction in poly(I:C)-treated and gene-silenced HCT-116 cells. Cells were pre-treated with siRNA (75 nM) to achieve gene-silencing for TLR3 and MAVS. IFN-β gene induction was measured via quantitative real-time PCR analysis and compared to baseline GAPDH gene expression levels. All samples were normalized to mock-treated HCT-116 cells with no siRNA pre-treatment. Poly(I:C) was prepared at a concentration of 10μg/mL for culture media treatment, and at a concentration of 2μg for transfection. All RNA samples were harvested 6 hours post-poly(I:C)-treatment. Differential levels of induction were observed for TLR3-deficient and MAVS-deficient cells. Values are mean ± s.d. from 3 experimental replicates per treatment.

(A) IFN-β gene induction in poly(I:C)-treated, gene-silenced HCT-116 samples. Poly(I:C) [10μg/mL] was mixed into cell culture media to simulate the presence of extracellular dsRNA.

(B) IFN-β gene induction in poly(I:C)-treated, gene-silenced HCT-116 samples. Poly(I:C) [2μg] was transfected into HCT-116 cells using Lipofectamine 2000 (Invitrogen) to mimic the presence of intracellular dsRNA.

(A)

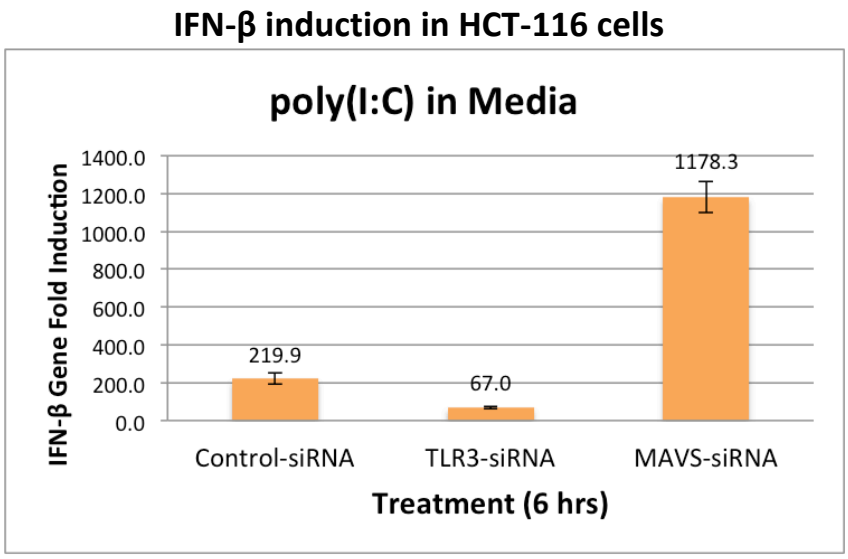
IFN-β induction in HCT-116 cells
poly(I:C) in Media
IFN-β Gene Fold Induction
1400.0
1200.0
1000.0
800.0
600.0
400.0
200.0
0.0
219.9
67.0
1178.3
Control-siRNA
TLR3-siRNA
MAVS-siRNA
Treatment (6 hrs)

(B)

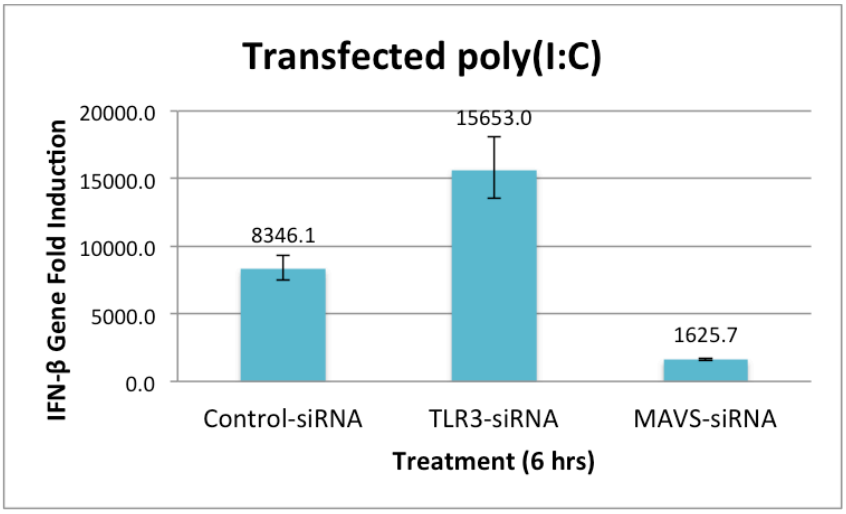
IFN-β induction in HCT-116 cells
Transfected poly(I:C)
IFN-β Gene Fold Induction
20000.0
15000.0
10000.0
5000.0
0.0
8346.1
15653.0
1625.7
Control-siRNA
TLR3-siRNA
MAVS-siRNA
Treatment (6 hrs)

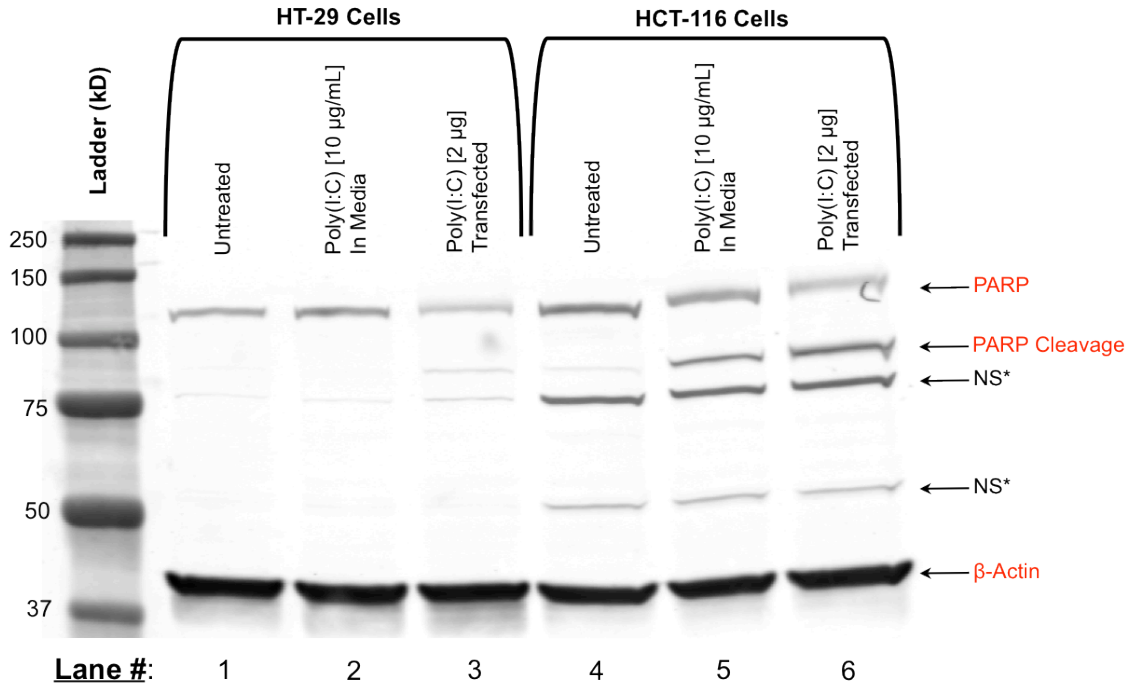

Figure 3. PARP-cleavage in poly(I:C)-treated HT-29 and HCT-116 cells. HT-29 and HCT-116 cell lines were treated with LMW poly(I:C) prepared at 10µg/mL for culture media treatment (extracellular) and at 2µg for transfection (intracellular). All protein extract samples were harvested 24 h post-treatment. Nitrocellulose membrane was probed with mouse anti-PARP primary antibody overnight, washed 3 times with PBS-0.05% Tween* 20 (Fisher Scientific) after which goat anti-mouse secondary antibody was added for 2 h. Western blot was visualized using a LI-COR Odyssey imager, and is representative of 2 independent experiments. *NS: Non-specific.

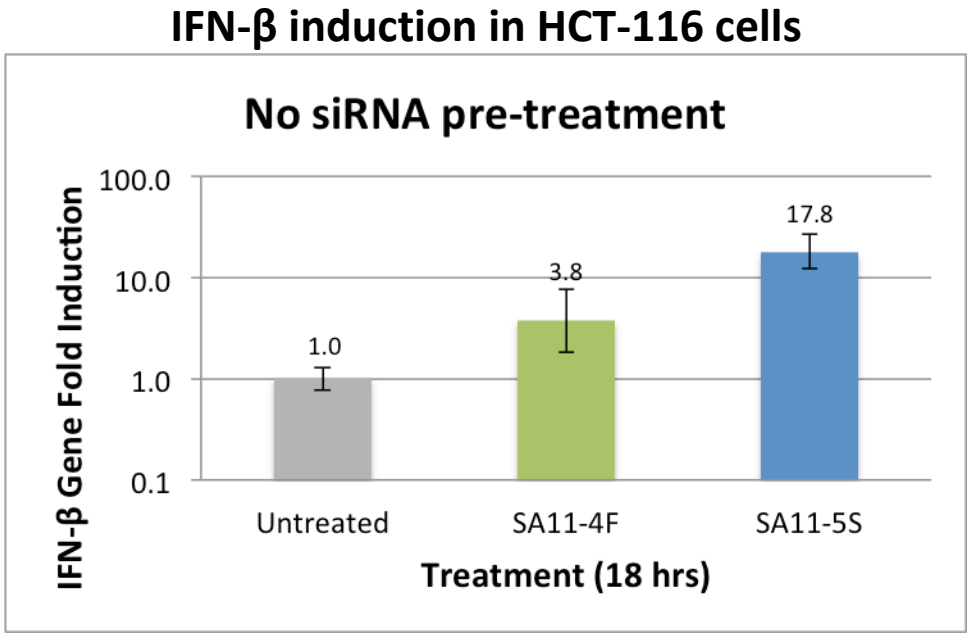

Figure 4. Differential IFN-β induction levels in SA11-4F- and SA11-5S-infected HCT-116 cells. HCT-116 cells were infected with both SA11-4F and SA11-5S rotavirus strains at an MOI of 5. HCT-116 samples were not pre-treated with siRNA to achieve gene knockdown, and all RNA samples were harvested 18-hours post-infection, and IFN-β gene induction levels were measured using quantitative real-time PCR analysis. IFN-β induction was compared against baseline GAPDH gene expression levels. Values are mean ± s.d. from 2 independent experiments conducted in triplicates.

Figure 5. IFN-β gene induction in rotavirus-infected, gene-silenced HCT-116 cells. Cells were pre-treated with siRNA (75 nM) to achieve gene-knockdown in TLR3 and MAVS. HCT-116 cells were infected with SA11-4F and SA11-5S rotavirus strains at an MOI of 5. All RNA samples were harvested 18 hours post-infection. IFN-β gene induction levels were measured by quantitative real-time PCR analysis and were compared to baseline GAPDH gene expression levels. All samples were normalized to mock HCT-116 cells with no siRNA pre-treatment. Values are mean ± s.d. from 2 independent experiments conducted in triplicates.

(A) IFN-β gene induction in SA11-4F-infected (MOI 5), gene-silenced HCT-116 samples.

(B) IFN-β gene induction in SA11-5S-infected (MOI 5), gene-silenced HCT-116 samples.

(A)

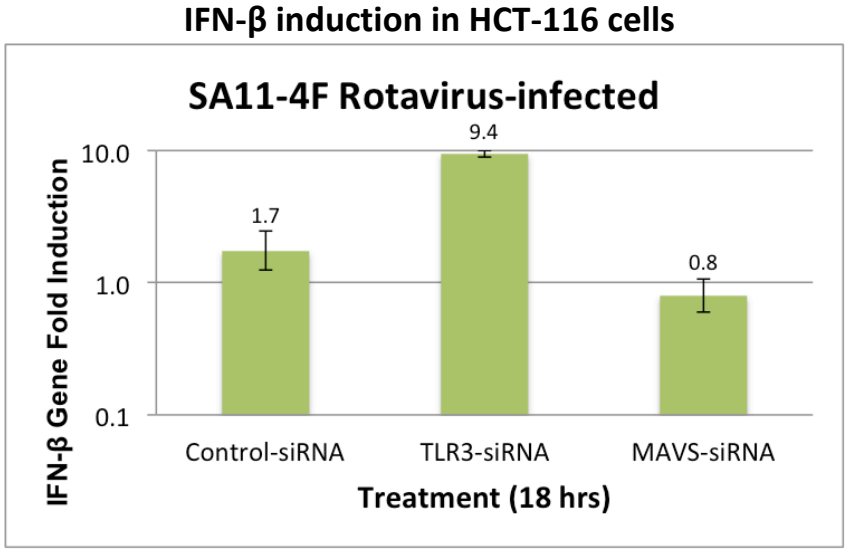
IFN-β induction in HCT-116 cells
SA11-4F Rotavirus-infected
IFN-β Gene Fold Induction
10.0
1.0
0.1
1.7
9.4
0.8
Control-siRNA
TLR3-siRNA
MAVS-siRNA
Treatment (18 hrs)

(B)

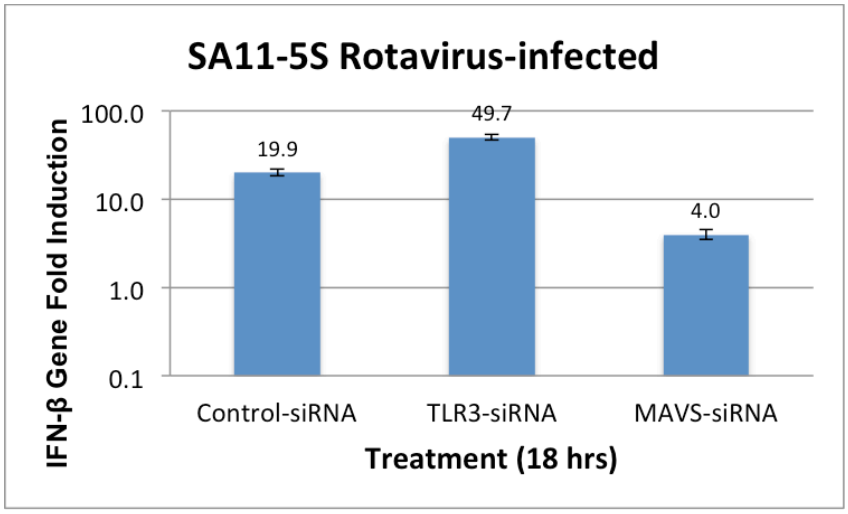
IFN-β induction in HCT-116 cells
SA11-5S Rotavirus-infected
IFN-β Gene Fold Induction
100.0
10.0
1.0
0.1
19.9
49.7
4.0
Control-siRNA
TLR3-siRNA
MAVS-siRNA
Treatment (18 hrs)

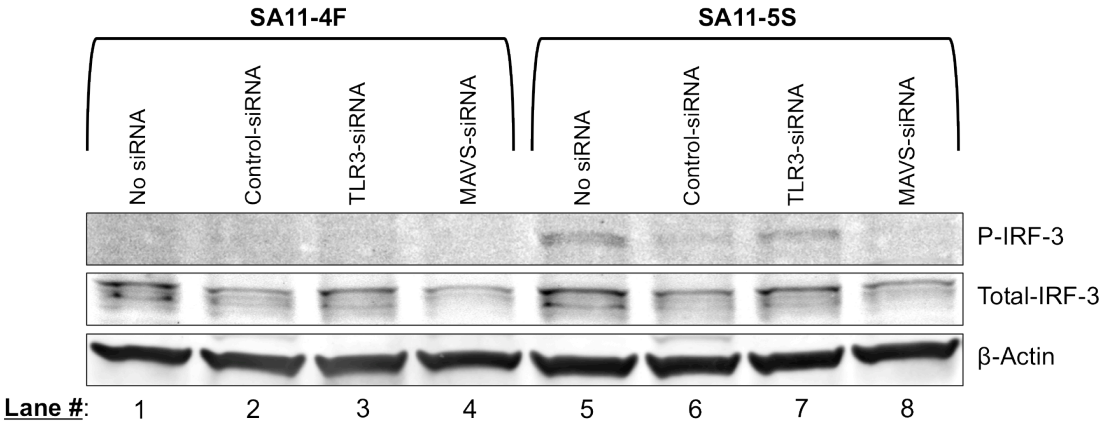

Figure 6. IRF-3 phosphorylation in rotavirus-infected HCT-116 cells. Cells were pre-treated with siRNA (75 nM) to achieve gene-silencing in TLR3 and MAVS. SA11-4F and SA11-5S rotavirus strains were used to infect HCT-116 cells at an MOI of 5. Protein extract samples were harvested 36 hours post-infection for western blot analysis. Total- and phosphorylated-IRF3 levels in rotavirus-infected HCT-116 samples are shown. β-actin, a housekeeping gene, was used as a loading control and showed consistent loading of samples. Western blot was visualized using a LI-COR Odyssey imager, and is representative of 2 independent experiments.

Figure 7. MAVS protein levels in various treatment conditions for HCT-116 cells. Gene-knockdown for TLR3 and MAVS was achieved using 75 nM of TLR3-siRNA and MAVS-siRNA, respectively. LMW Poly(I:C) was prepared at 10μg/mL and mixed with culture media, and SA11-4F and SA11-5S strains of rotavirus were used for infection at an MOI of 5. All samples, including rotavirus-infected and poly(I:C)-treated, were harvested 36-hours post-treatment. Goat anti-rabbit IgG antibody was used to detect MAVS via western blot. β-Actin, a housekeeping gene, was used as a loading control and showed consistent loading of samples. Western blot was visualized using a LI-COR Odyssey imager, and is representative of 2 independent experiments. *NS: Non-specific.

(A) MAVS protein levels in control HCT-116 protein extract samples (no siRNA and control-siRNA).

(B) MAVS protein levels in TLR3- and MAVS-deficient HCT-116 protein extract samples.

(A)

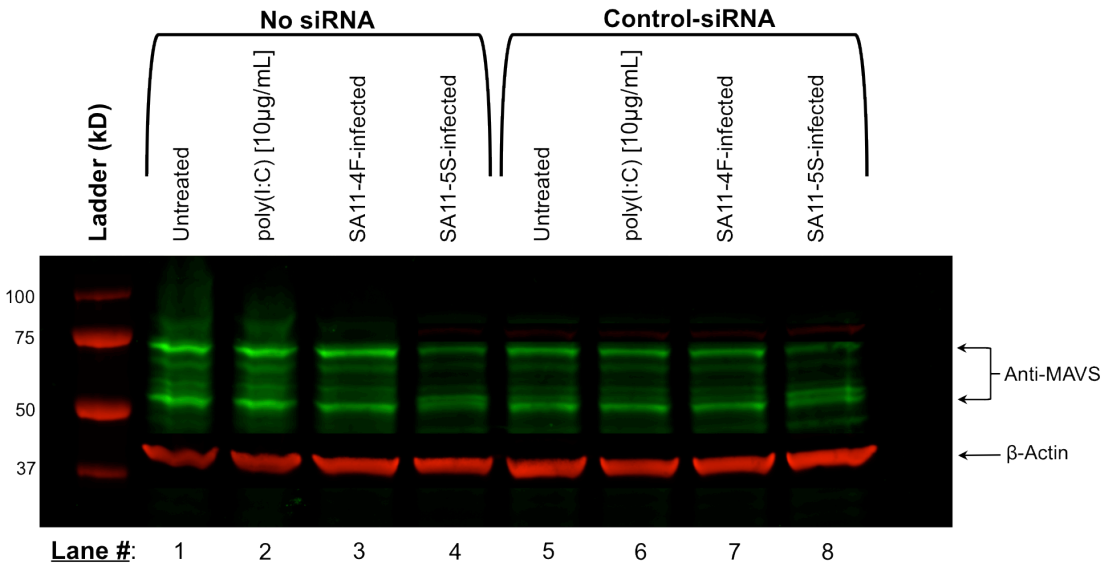
No siRNA
Control-siRNA
Ladder (kD)
Untreated
poly(I:C) [10µg/mL]
SA11-4F-infected
SA11-5S-infected
Untreated
poly(I:C) [10µg/mL]
SA11-4F-infected
SA11-5S-infected
100
75
50
37
Anti-MAVS
β-Actin
Lane #: 1 2 3 4 5 6 7 8

(B)

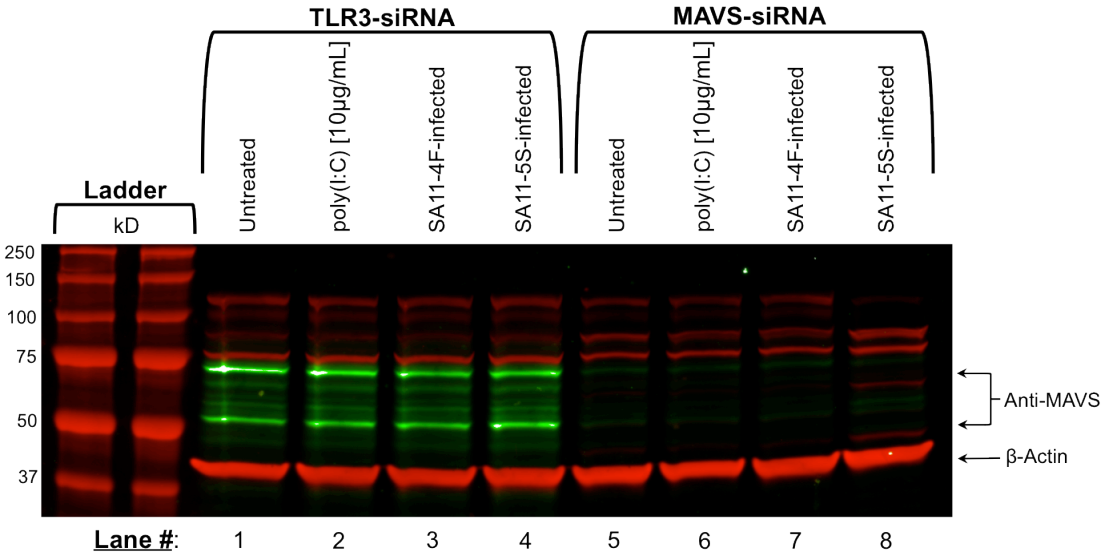
TLR3-siRNA
MAVS-siRNA
Ladder
kD
Untreated
poly(I:C) [10µg/mL]
SA11-4F-infected
SA11-5S-infected
Untreated
poly(I:C) [10µg/mL]
SA11-4F-infected
SA11-5S-infected
250
150
100
75
50
37
Anti-MAVS
β-Actin
Lane #: 1 2 3 4 5 6 7 8

Figure 8. PARP-cleavage in rotavirus-infected and poly(I:C)-treated HCT-116 cells. Gene-knockdown was achieved using 75 nM of TLR3-siRNA and MAVS-siRNA for TLR3 and MAVS, respectively. LMW Poly(I:C) was prepared at 10 μg/mL for mixing with culture media, and SA11-4F and SA11-5S strains of rotavirus were used for infection at an MOI of 5. All samples, including rotavirus-infected and poly(I:C)-treated, were harvested 36-hours post-treatment. β-Actin, a housekeeping gene, was used as a loading control and showed consistent loading of samples. Western blot was visualized using a LI-COR Odyssey imager, and is representative of 2 independent experiments. *NS: Non-Specific.

(A)

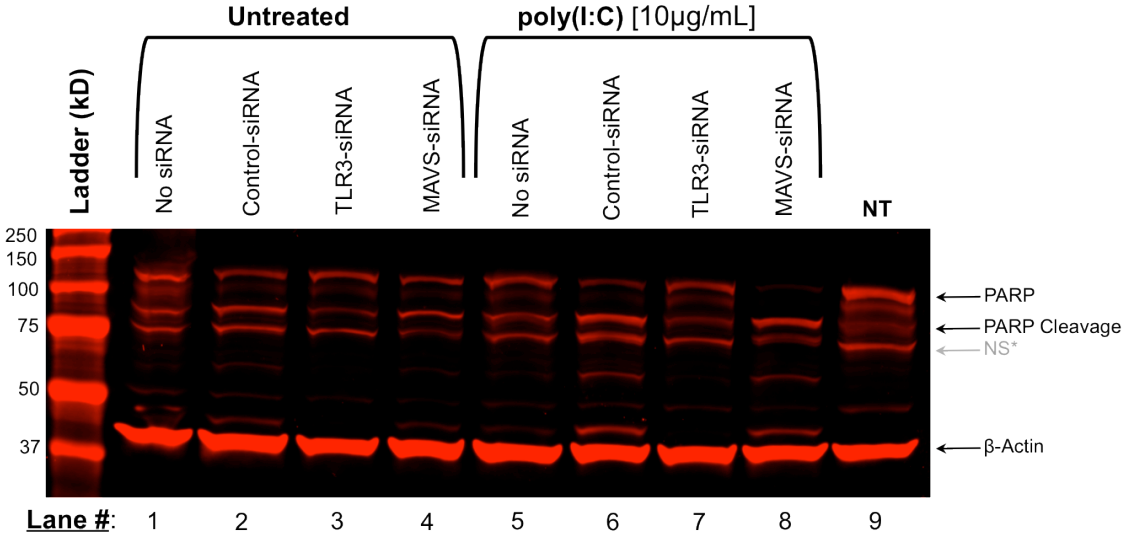
Untreated
poly(I:C) [10µg/mL]
Ladder (kD)
No siRNA
Control-siRNA
TLR3-siRNA
MAVS-siRNA
No siRNA
Control-siRNA
TLR3-siRNA
MAVS-siRNA
NT
250
150
100
75
50
37
PARP
PARP Cleavage
NS*
β-Actin
Lane #: 1 2 3 4 5 6 7 8 9

(B)

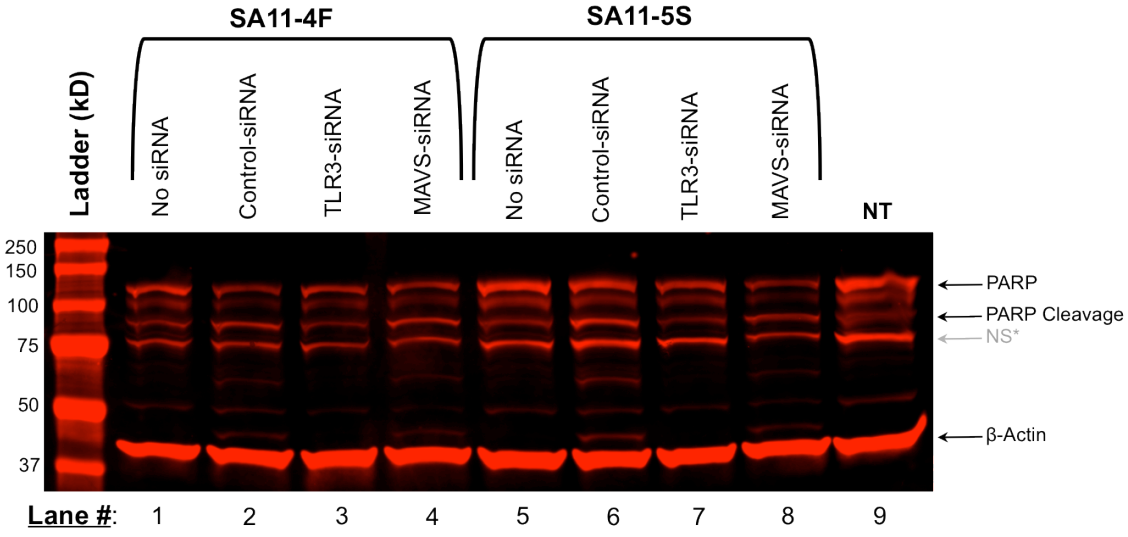
SA11-4F
SA11-5S
Ladder (kD)
No siRNA
Control-siRNA
TLR3-siRNA
MAVS-siRNA
No siRNA
Control-siRNA
TLR3-siRNA
MAVS-siRNA
NT
250
150
100
75
50
37
PARP
PARP Cleavage
NS*
β-Actin
Lane #: 1 2 3 4 5 6 7 8 9

Figure 9. Plaque assay with MA104 cells, using viral supernatant from SA11-5S-infected HCT-116 cells. A plaque assay was performed with MA104 cells using viral supernatant obtained from SA11-5S rotavirus-infected HCT-116 cells pre-treated with no siRNA, control-siRNA, TLR3-siRNA or MAVS-siRNA at 75 nM. Plaques were counted for each respective treatment condition, 48 hours post-infection.

(A) Visualization of plaques for the respective treatment conditions, including no siRNA, control-siRNA, TLR3-siRNA, and MAVS-siRNA, respectively.

(B) Quantification of plaque formation in SA11-5S rotavirus-infected MA104 cells for no siRNA, control-siRNA, TLR3-siRNA, and MAVS-siRNA conditions.

(A)

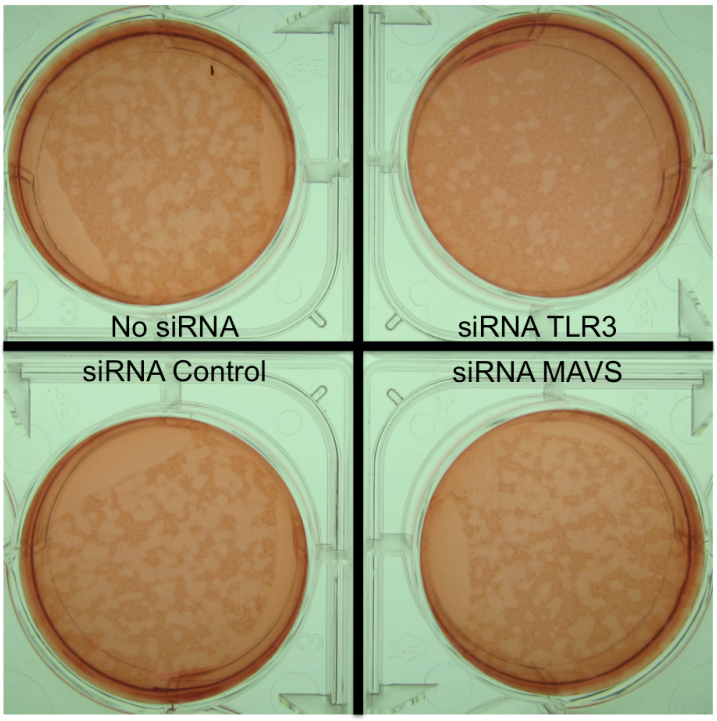
No siRNA
siRNA TLR3
siRNA Control
siRNA MAVS

(B)

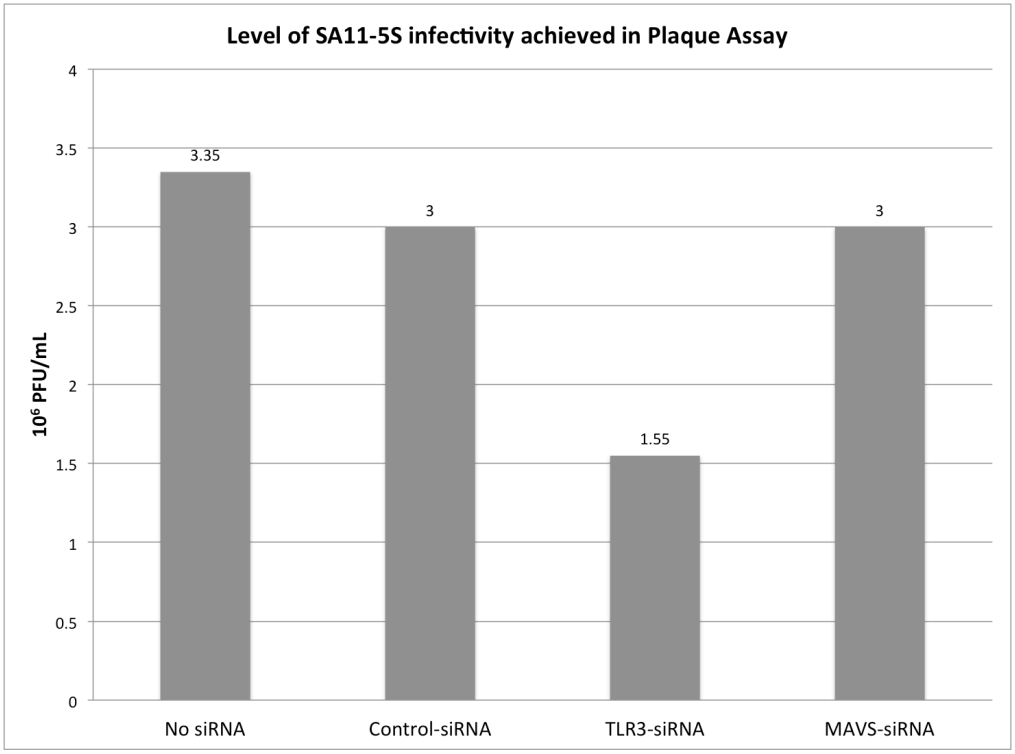
Level of SA11-5S infectivity achieved in Plaque Assay
10⁶ PFU/mL
4
3.5
3
2.5
2
1.5
1
0.5
0
3.35
3
1.55
3
No siRNA
Control-siRNA
TLR3-siRNA
MAVS-siRNA

DISCUSSION

Extracellular & intracellular dual-dependent signaling in HCT-116 cells

A previous study conducted by the Kagnoff Laboratory found that HT-29 and HCA-7 cell lines relied on intracellular signaling via the RIG-I/Mda-5/MAVS pathway to respond to rotavirus (Broquet, *et al*., 2011). Recently another group showed that TLR3-signaling is also important *in vivo* for murine rotavirus-infected mice (Pott, *et al.*, 2012). Previous research conducted on Influenza A virus (IAV) has suggested important roles for both TLR3-dependent and MAVS-dependent signaling in eliciting innate immune responses in IAV-infected human respiratory epithelial cells (Le Goffic, *et al.*, 2007). This points to the potential importance of both signaling pathways in generating an innate immune response in IECs as well. However, dual-reliance on both RLR- and TLR3-signaling for IFN-expression in rotavirus-infected IECs has not been clearly demonstrated *in vitro* or *in vivo*. We have now demonstrated that HCT-116 cells have the ability to generate an innate immune response through both the extracellular, TLR3-dependent, and intracellular, MAVS-dependent, pathways.

Comparable PARP-cleavage levels for extracellular & intracellular signaling

The HCT-116 cell line could help elucidate the importance of This observed dual-dependency in HCT-116 cells was seen for IFN-β induction and further supported PARP-cleavage analysis for apoptosis, where introduction of both extracellular and intracellular dsRNA resulted in comparable levels of PARP-

cleavage. Conversely, such a dual-dependency was not observed in HT-29 cells, in which PARP-cleavage was only observed for samples exposed to intracellular dsRNA [transfected poly(I:C)]. Moreover, PARP cleavage levels were much lower in poly(I:C)-treated HT-29 cells compared to poly(I:C)-treated HCT-116 cells overall, possibly suggesting the requirement for a longer poly(I:C) incubation period for HT-29 cells.

MAVS and TLR3 dependency in rotavirus-infected HCT-116 cells

Rotavirus-infected HCT-116 cells yielded trends consistent to poly(I:C)-treated HCT-116 cells in IFN-β induction, but also provided more interesting results. The two rotavirus strains that I used, SA11-4F and SA11-5S, differ in their encoded NSP1 proteins, with SA11-4F NSP1 being a wild-type version and SA11-5S NSP1 being a C-terminal truncated version. Though SA11-5S rotavirus yielded more overall IFN-β induction, consistent induction trends were observed for IFN-β induction between SA11-4F- and SA11-5S-infected HCT-116 cells upon TLR3- or MAVS-silencing. MAVS-silencing for both SA11-4F- and SA11-5S-infected HCT-116 cells resulted in significantly suppressed IFN-β induction levels. This demonstrated a MAVS-dependency in IFN-β induction. Further, MAVS-silenced samples yielded no IRF-3-phosphorylation when levels of IRF-3 activation in SA11-5S-infected HCT-116 cells were analyzed.

On the other hand, TLR3-silencing in SA11-5S-infected HCT-116 cells yielded nearly 2.5-fold more in IFN-β response, compared to SA11-5S-infected control-

siRNA-treated samples. Moreover, TLR3-silenced HCT-116 cells also exhibited higher levels of IRF-3-phosphorylation than samples treated with control-siRNA. These observations suggest that TLR3-signaling may negatively regulate MAVS-dependent signaling. Interestingly, along with the robust IFN-β response observed in TLR3-silenced HCT-116 cells upon SA11-5S rotavirus infection, there appeared to be higher MAVS protein levels as well. When comparing MAVS levels among SA11-5S-infected HCT-116 cells, samples pre-treated with TLR3-siRNA resulted in no reduction in MAVS, whereas samples pre-treated with no siRNA, control-siRNA or MAVS-siRNA, yielded noticeably lower levels of MAVS. Because this reduction in MAVS could be due to cell death, we analyzed apoptosis in SA11-5S-infected HCT-116 cells and found that the increase in IFN-β induction following TLR3-knockdown coincided with reduced levels of PARP-cleavage.

Loss of TLR3 in SA11-5S-infected HCT-116 cells yielded increased levels of IFN-β induction, increased levels of IRF-3-phosphorylation, less apoptosis, as well as higher levels of MAVS. Furthermore, a plaque assay performed in MA104 cells, by using viral supernatant obtained from SA11-5S-infected HCT-116 cells, resulted in approximately half the number of plaques in TLR3-silenced samples, indicating a biological effect of TLR3 knockdown on viral replication. This correlates to the observations made in a prior *in vivo* study performed in murine rotavirus-infected mice. The group showed that upon rotavirus infection, TLR3-signaling resulted in severe small intestinal damage and disruption to mucosal homeostasis (Zhou, *et al.*, 2007).

Despite our observations, there seems to be various limitations to the apoptosis assay with rotavirus that was conducted. Mainly, while utilizing siRNA to achieve gene-silencing, high PARP-cleavage background was consistently observed for cells transfected with no siRNA, control-siRNA and MAVS-siRNA. PARP-cleavage data obtained from rotavirus-infected HCT-116 cells was therefore equivocal in comparison to the PARP-cleavage data obtained from poly(I:C)-treated HCT-116 cells. Furthermore, SA11-4F- and SA11-5S-infected cells did not result in significant differential levels in PARP-cleavage. In future studies, an annexin V and propidium iodide assay will be used to provide a more robust approach to studying apoptosis, which will allow for the identification of cells at different stages of apoptosis and necrosis.

If in fact it remains true that there is no difference between SA11-4F and SA11-5S apoptosis induction after using another assay for cell death, there are several potential explanations. As mentioned before, activated IRF-3 has been demonstrated to harbor a dual-functionality; in addition to IRF-3's ability to translocate into the nucleus to influence expression of antiviral genes, it also mediates a mitochondrial-dependent apoptotic response that is entirely separate from its role as a transcription factor (Chattopadhyay, *et al*., 2010). The mitochondrial signaling downstream of IRF-3 is mediated by Bcl-2-associated X protein (Bax), which aids activated-IRF-3 in its translocation to the mitochondria, leading to a subsequent release of Cytochrome C to initiate the apoptotic process (Chattopadhyay, *et al*., 2010). A recent study suggested that the inhibitory effects of

NSP1 could be partially responsible for preventing apoptotic effects observed in intestinal epithelial cells following rotavirus infection (Bagchi, *et al*., 2010). This would therein help encourage rotavirus proliferation within the host upon infection. Therefore, we expected more PARP-cleavage to occur in SA11-5S-infected HCT-116 samples than in SA11-4F-infected HCT-116 samples because we suspected the truncated SA11-5S NSP1 would not be able to engage in IRF-3 inhibition. However, since SA11-5S NSP1 is only missing 17 amino acids on its C-terminus, it may still harbor some interactive capabilities with IRF-3, as well as some anti-apoptotic effects. This would explain the similar levels of PARP-cleavage that I observed between SA11-4F- and SA11-5S-infected HCT-116 cells, as opposed to more PARP-cleavage in SA11-5S-infected samples. While it was previously reported that the entire NSP1 IRF-3 binding domain is needed to prevent IRF-3 nuclear translocation, which is required for it to act as a transcription factor (Barro & Patton, 2005), it remains possible that the entire NSP1 IRF-3 binding domain may not be needed for it to prevent IRF-3 interaction with Bax.

Evidence from another research group has shown that NSP1 is important for countering apoptosis during infection in other IEC lines, such as Caco-2 (Barro & Patton, 2007), and there is potential for it being the case in the HCT-116 cell line as well. In hopes of clarifying these ambiguities, I have utilized DNA cloning strategies to construct recombinant plasmids containing the NSP1 gene for SA11-4F rotavirus and RRV rotavirus, engineered into recombinant plasmids containing an Anti-Xpress epitope tag for future experimental analysis. Moreover, previous studies have

shown that NSP1 degrades IRF-3 by inhibition of proteasomes (Barro & Patton, 2005; Barro & Patton, 2007; Graff, *et al.*, 2009). By introducing these NSP1 plasmids into mammalian cells via transfection to assay NSP1's effect on dsRNA-induced cell death, we will hopefully be able to better understand whether NSP1 modulates cell death during rotavirus infection.

Limitations Surrounding HCT-116 Cells for understanding IECs

Although interesting results were achieved through these series of experiments in the HCT-116 cell line, there may be certain limitations in HCT-116's relevance to small intestinal epithelial cell studies. For one, the HCT-116 cell line is derived from the colon as opposed to the small intestine, and secondly, it is a poorly differentiated *in vitro* cell line (Hoosein, *et al*., 1989). However, it shows promise in being a useful *in vitro* model for understanding IEC dual-dependency in dsRNA-signaling because it exhibits TLR3-dependency, which is not commonly observed in well-differentiated IEC lines. HCT-116 cells also express wild-type p53, another atypically observed feature among differentiated colorectal carcinoma IEC lines (El-Deiry, *et al*., 1994; Take, *et al*., 1996). The relevance of the HCT-116 cell line to functional small intestinal epithelial cell lines thus remains equivocal and warrants ongoing investigations.

Future Directions

Through my work as part of this Master's project, I observed HCT-116's potential reliance in both extracellular and intracellular dsRNA signaling through the TLR3/TRIF and RIG-I/Mda-5/MAVS pathways. To better characterize this dual-dependency in generating an IFN-response, it would be important for future HCT-116 *in vitro* studies to be carried out in parallel with a control IEC line, such as HCA-7 (Broquet, *et al*., 2011), a well-characterized *in vitro* IEC cell line.

Analysis of the TRIF adaptor protein could help elucidate the role of extracellular dsRNA-signaling via TLR3 in HCT-116 cells. By achieving TRIF knockdown via siRNA gene-silencing approaches, TRIF's role in inducing IFN-expression, as well as its importance in dsRNA signaling relative to its TLR3 counterpart, may be determined via RNA isolation and quantitative real-time PCR (qPCR) analysis. Additionally, ELISA protein assays may also be conducted to analyze differences in IFN protein expression levels for various gene knockdown conditions that include MAVS-silenced, TLR3-silenced, and TRIF-silenced HCT-116 cells. In addition to these future HCT-116 *in vitro* studies, *in vivo* approaches towards characterizing the extracellular and intracellular signaling pathways in IECs can also be performed. TLR3-, TRIF-, and MAVS-knockout mice can be infected with different strains of murine rotaviruses, which would allow us to further understand the relevancy of the extracellular (TLR3/TRIF-dependent) and intracellular (RIG-I/Mda-5/MAVS-dependent) signaling pathways for summoning innate immune responses in IECs.

MATERIALS AND METHODS

Culturing and Seeding HT-29 & HCT-116 Cells

The two human small intestinal cell lines used, HT-29 and HCT-116, were grown in RPMI-1640 cell culture media supplemented with 10% heat-inactivated FBS supplemented with 2mM L-glutamine, and 1% penicillin/streptomycin antibiotic. IECs were incubated in a 95% air/5% CO_2 environment at a constant temperature of 37° C. The cells were cultured in 75 cm^2 flasks (Corning), and were trypsinized with 0.25% Trypsin (with EDTA) upon reaching 80% confluency. Cells were subsequently seeded at a density of 7.0 x 10^5 cells/mL into 24-well commercially conditioned plates (Corning), and allowed to grow overnight (approximately 24 hours) in a humidified 95% air/5% CO_2 incubator at 37°C.

Gene-silencing in HCT-116 Cells via siRNA

DharmaFECT transfection reagent, purchased through Thermo Scientific, was used to introduce small interfering RNA (siRNA) into HCT-116 cells to knockdown the TLR3 and MAVS (IPS-I) genes. Control-siRNA, TLR3-siRNA, and MAVS-siRNA oligonucleotides were purchased commercially through Dharmacon and were used as described previously (Hirata, *et al*., 2007). Prior to siRNA transfection, wells were pre-incubated with 200 µl of RPMI-1640 media, containing 10% heat-inactivated FBS and 2mM L-glutamine without penicillin/streptomycin. The DharmaFect transfection protocol was followed after preparing 75 nM concentration of siRNA for transfection. siRNA transfection complexes were

allowed to form for 20 minutes, and 100 µl of media containing transfection complex was placed drop-wise onto each well. The transfected cells were allowed to incubate in a humidified 95% air/5% CO_2 environment at 37°C for 48 hours before the desired poly(I:C) treatments or rotavirus infections were conducted.

Rotavirus Infection of HCT-116 Cells

Rotavirus SA11-5S and SA11-4F strains were used as part of this study (Patton, *et al.*, 2001). Viruses were activated in 0.2 µg/ml diluted trypsin for 1 hour at 37° C. After trypsin activation, viruses were diluted to the desired volume, and 500 µl of virus solution was placed drop-wise onto fully confluent wells of HCT-116 cells to achieve infection at an MOI of 5. Samples were allowed to incubate for 1 h in 95% air/5% CO_2 at 37° C. Virus supernatant was removed, and 500 µl of fresh RPMI-1640 media (containing no FBS and no penicillin/streptomycin) was added to each respective well for 24- or 36-hour incubations.

Poly(I:C)-Treatment of HCT-116 Cells via Cell Culture Media

Cultured cells were allowed to grow to 90% confluency in preparation for synthetic dsRNA treatment. Low molecular weight (LMW) and high molecular weight (HMW) polyinosidylic-polycytidylic acid [poly(I:C)] [InvivoGen] were prepared at a concentration of 10µg/mL using serum-free RPMI media without antibiotics. For in media treatment (extracellular introduction of dsRNA), 500 µl of

diluted poly(I:C) was placed drop-wise onto each well, and poly(I:C) treatment lasted 6 hours for RNA samples, and 18 hours for protein lysate samples.

Poly(I:C)-Treatment of HCT-116 Cells via Transfection

Cultured cells were allowed to grow to 90% confluency in preparation for synthetic dsRNA treatment. 200 µl of new RPMI-1640 media was placed into each cell culture well prior to application of poly(I:C)-transfection complexes. LMW and HMW poly(I:C) [InvivoGen] were prepared at a concentration of 2 µg for transfection (intracellular dsRNA introduction). Lipofectamine 2000 (Invitrogen) transfection reagent and serum-free RPMI-1640 media without antibiotics were used. For each well reaction, 2 µg of poly(I:C) was mixed in 100 µl of transfectaGRO Reduced Serum Medium (Cellgro, Corning) and allowed to sit for 5 min at room temperature. 3 µl of Lipofectamine 2000 was mixed with 100 µl of transfectaGRO Reduced Serum Medium (Cellgro, Corning) and allowed to sit for 5 min at room temperature. The 2 mixtures were subsequently combined, and gently pipetted up and down to mix, followed by a 30-min room temperature incubation period to allow formation of transfection complexes. Following complex formation, 200 µl of complexes were added drop-wise onto each cell culture well. Transfection was allowed to occur for 6 hours prior to removal of transfection media, and supplementation of 400 µl of fresh RPMI-1640 media to each transfection complex-treated well. RNA samples were isolated 18 hours post-treatment, and protein samples were harvested 24 hours post-treatment.

RNA Extraction and Quantitative Real-time PCR Analysis

RNA was harvested from the rotavirus-infected HCT-116 cells at an 18 hour time-point, and purified using an RNeasy Mini Kit from Qiagen (Valencia, CA). Likewise, RNA from poly(I:C)-treated HCT-116 cells was purified using an RNeasy Mini Kit (Qiagen), but instead was harvested from the cells at a 6 hour time-point. The RNeasy Mini Kit protocol provided by Qiagen was followed and the optional on-column DNase I (Qiagen) treatment was also performed. Sample absorbances for isolated RNA samples were subsequently taken using a NanoDrop 2000c apparatus (Thermo Scientific) to determine nucleic acid concentration. Utilizing an iScript Reverse Transcription kit from BioRad, 1 μg of purified RNA was used to synthesize complementary DNA (cDNA). To measure gene induction, quantitative real-time PCR analysis was carried out by mixing reverse-transcribed cDNA with respective forward and reverse primers for the gene of interest (ie. IFN-β), and with 2 X SYBR green Master mix from Applied Biosystems (Foster City, CA). The GAPDH gene, a housekeeping gene in mammalian cells, was used as a control for comparing IFN-β gene fold induction to GAPDH gene baseline expression levels. The real-time PCR cycles were carried out in an ABI Prism 7000 Sequence Detection System from Applied Biosystems, and were allotted 5 minutes at 95° C for denaturation, followed by 40 cycles of DNA amplification with 30 seconds at 95° C, and 30 seconds at 60° C.

Immunoblot Analysis

HCT-116 cells in 12-well plates were washed with PBS, and were harvested 36 hours post-treatment with 100 µl of protein lysis buffer (50mM Tris HCl, pH 8.0, 1% Nonidet P40, 150 mM NaCL, 100 mg/ml leupeptin, 1 mM PMSF, 5 mM $NaVO_4$) containing protease inhibitor. Cell lysates were spun at 10,000 RPM for 5 min at 4°C. Each aliquotted sample was mixed with 4X SDS loading buffer (containing DTT), boiled for 5 minutes, and loaded on a 12% Mini-PROTEAN TGX Precast Gel (BioRad) at constant 200V for 30 minutes. Running buffer was prepared using 100 mL of a 10X TG-SDS Running Buffer (LI-COR), mixed with 900 mL of Millipore-purified water. Transfer Buffer was prepared using 100 mL of a 10X TG Transfer Buffer (LI-COR), plus 100 mL of methanol, and 800 mL of Millipore-purified water. Separated proteins were transferred onto Odyssey Nitrocellulose Membranes (LI-COR) at 120V, and were subsequently blocked for 2 hours using Odyssey Blocking Buffer (LI-COR). Primary antibodies for PARP (Cell Signaling Technology), P-IRF-3 (Cell Signaling Technology), as well as β-actin (Sigma-Aldrich), were incubated with the nitrocellulose overnight. Anti-MAVS (Bethyl Laboratories) was also used as a primary antibody for some nitrocellulose membranes as part of this project. Following primary antibody incubation, nitrocellulose membranes were washed 3 times, 10 min each, with 1X PBS containing 0.05% Tween* 20 (Fisher Scientific), followed by one 10-min wash with 1X PBS, and a 10-min Odyssey Blocking Buffer (LI-COR) wash. Blots were subsequently probed with secondary antibodies, IRDye 680RD goat anti-mouse IgG antibody, as well as IRDye 800CW goat anti-rabbit IgG antibody, both obtained from LI-COR. After secondary antibody incubation, three

10-min PBS-Tween washes were performed, followed by another 10-min PBS wash. Western blots were subsequently visualized using a LI-COR Odyssey Infrared Imaging System.

Viral Plaque Assay

Plaque assay was performed with using MA104 cultured cells for each plaque assay according to the protocol of Arnold *et al.*, 2009. MA104 cells were pre-cultured in 150 cm^2 flasks (Corning), and placed into a 37°C, 5% CO_2, humidified incubator until full-confluency was achieved. MA104 cells were seeded into four 6-well plates (Corning) at a density of 3.0×10^5 cells/well and were allowed to grow for 4 days in the humidified incubator. Viral media obtained from SA11-5S rotavirus-infected HCT-116 cells were saved, and were activated by adding 4 µl of 0.5 mg/mL trypsin to 100 µl of viral media. Virus was subsequently placed into a 37°C water bath for 1 hour. After virus activation, serial dilutions were completed by adding 900 µl of 1X 199 media, containing no serum, into the first dilution tube, followed by 1080 µl of media into six other dilution tubes. 100 µl of activated virus was added to the first dilution tube, and 120 µl of the diluted first tube, was transferred to the second, and so forth in order to achieve an endpoint of 10^{-7}. Following that, 1 mL of each completed serial dilution was placed into one of each of the 6-well plates. Each plate was subsequently left in the humidified incubator and left for incubation for 1 hour, with gentle rocking every 15 minutes. For each plaque assay, an agarose overlay was prepared by warming 12 mL of 2X 199 media with no

serum, with 0.18 g of Agarose LE filled to 15 mL of autoclaved water. The mixture was boiled, and temporarily stored in a 42°C water bath. Pancreatin facilitator was prepared at 5 mg/mL, while DEAE dextran facilitator was prepared at 10 mg/mL. 39 µl of Pancreatin and 30 µl DEAE was added to 12mL 2X 199 media, and was subsequently stored at 42°C as well. After the 1 h-long incubation, virus was removed from wells in the order of most dilute to most concentrated. 12 mL of agarose was combined with 12 mL of media containing facilitators, followed by a quick mix. Immediately following this, 3 mL of agarose/medium overlay was applied via the side of each plaque assay well. Agarose/medium layer was allowed to cool at room temperature, and was left inverted in the humidified incubator overnight. A second overlay was likewise prepared in a 1:1 ratio for agarose and medium, but containing 50 mg/mL of neutral red. 7.5 mL of agarose was mixed with 7.5 mL 2X 199 media containing neutral red, and 2 mL of agarose/medium overlay was then distributed into each plaque assay well. Plaques were allowed to form for 3 days in the humidified incubator after application of the second overlay and prior to visualization on a light box.

Synthesis of NSP1 Recombinant Plasmids

MA104 rhesus monkey kidney cells were first cultured as described by Arnold, *et al*., 2009. Confluent MA104 cells were infected with the respective strains of rotavirus (SA11-4F and SA11-5S) for 4 days to allow rotavirus amplification. Viral media was subsequently freeze-thawed a total of 3 times, and then spun down

twice for 10 minutes each at 10,000 RPM on a table-top centrifuge (Sorvall RT 6000B). Samples were subsequently spun down using a high-speed ultra-centrifuge (Beckman L7-65) for 3 hours at 25,000 RPM after which RNA was isolated from rotaviral supernatant using TriZol RNA extraction. Reverse transcription reactions were performed using an Omniscript Reverse Transcription kit (Qiagen) to obtain cDNA products. High-fidelity PCR reactions (Finnzymes Phusion kit, Thermo Scientific) were subsequently carried out. The NSP1 gene was amplified with NSP1 forward (5' TAC TGG TAC CAT GGC TAC TTT TAA AGA TGC ATG C 3') and reverse primers (5' TAG TTC TAG ATC AAA TTC CAG AAT TCT TCA TTT C 3') [ValueGene Inc.] with engineered Kpn-I and Xba-I sticky ends respectively. Kpn-I and Xba-I restriction enzymes were used to cleave the amplified NSP1 gene fragment as well as the multiple cloning site (MCS) of pcDNA3.1A DNA plasmid (Invitrogen). These insert and vector samples were subsequently run on a 1% agarose gel, and gel purified using a DNA Gel Extraction kit from Qiagen. A ligation was performed overnight with the amplified and restriction enzyme-digested NSP1 genes and plasmids. Following this, recombinant plasmids were sequenced by Eton BioSequencing (San Diego, CA).

REFERENCES

Akira, S. 2001. Toll-like receptors and innate immunity. *Adv. Immunol.* **78**:1-56.

Akira, S., and K. Takeda. 2004. Toll-like Receptor Signalling. *Nature Reviews Immunol.* **4**: 499-511.

Alexopoulou, L., A. C. Holt. R. Medzhitov, and R. A. Flavell. 2001. Recognition of double-stranded RNA and activation of NF-κB by Toll-like receptor 3. *Nature* **413**: 732-738.

Arnold, M., J. T. Patton, and S. M. McDonald. Culturing, Storage, and Quantification of Rotaviruses. 2009. *Current Protocols in Microbiology*. 15C.3.1-15C.3.24.

Bagchi, P., D. Dutta, S. Chattopadhyay, A. Mukherjee, U. C. Halder, S. Sarkar, N. Kobayashi, S. Komoto, K. Taniguchi, and M. Chawla-Sarkar. 2010. Rotavirus Nonstructural Protein 1 Suppresses Virus-Induced Cellular Apoptosis To Facilitate Viral Growth by Activating the Cell Survival Pathways during Early Stages of Infection. *J. Virol*. **84**: 6834-6845.

Barro, M., and J. T. Patton. 2005. Rotavirus nonstructural protein 1 subverts innate immune response by inducing degradation of IFN regulatory factor 3. *Proc. Natl. Acad. Sci. USA* **102**: 4114-4119.

Barro, M., and J. T. Patton: 2007. Rotavirus NSP1 inhibits expression of type I interferon by antagonizing the function of intereferon regulatory factors IRF-3, IRF5, and IRF7. *J. Virol.* **81**: 4473-4481.

Bartlett, A. V., A. J. Bednarz-Prashad, H. L. DuPont, and L. K. Pickering. 1987. Rotavirus Gastroenteritis. *Ann. Rev. Med.* **38**: 399-415.

Broquet, A., Y. Hirata, C. S. Mcallister, and M. F. Kagnoff. 2011. RIG-I/MDA5/MAVS Are Required To Signal a Protective IFN Response in Rotavirus-Infected Intestinal Epithelium. *J. Immunol*. **186**: 1618-1626.

Cario, E., and D. K. Podolsky. 2000. Differential alteration in intestinal epithelial cell expression of Toll-like receptor 3 (TLR3) and TLR4 in inflammatory bowel disease. *Infect. Immuno.* **68**: 7010-7017.

Chattopadhyay, S., J. T. Marques, M. Yamashita, K. L. Peters, K. Smith, A. Desai, B. R. G. Williams, and G. C. Sen. 2010. Viral apoptosis is induced by IRF-3-mediated activation of Bax. *EMBO J.* **29**: 1762-1773.

Chawla-Sarkar, M., D. J. Lindner, Y.-F. Liu, B. R. Williams, G. C. Sen, R. H. Silverman

and E. C. Borden. 2003. Apoptosis and interferons: Role of intereferon-stimulated genes as mediators of apoptosis. *Apoptosis* **8**: 237-249.

Ciarlet, M., and M. K. Estes. 2001. Interactions between rotavirus and gastrointestinal cells. *Curr. Opin. Microbiol*. **4**: 435-441.

Cohen, J. 1977. Ribonucleic acid polymerase activity associated with purified calf rotavirus. *J. Gen. Virol.* **36**:395-402.

El-Deiry, W. S., J. W. Harper, P. M. O'Connor, V. E. Velculescu, C. E. Canman, J. Jackman, J. A. Pietenpol, M. Burrell, D. E. Hill, Y. Wang, K. G. Wiman, W. E. Mercer, M. B. Kastan, K. W. Kohn, S. J. Elledge, K. W. Kinzler, and B. Vogelstein. 1994. *WAF1/CIP1* Is Induced in *p53*-mediated G_1 Arrest and Apoptosis. *Cancer Res.* **54**: 1169-1174.

Estes, M. K. and J. Cohen. 1989. Rotavirus Gene Structure and Function. *Microbiol Rev.* **53**: 410-449.

Fitzgerald, K. A., S. M. McWhirter, K. L. Faia, D. C. Rowe, E. Latz, D. T. Golenbock, A. J. Coyle, S. M. Liao, T. Maniatis. 2003. IKKε and TBK1 are essential components of the IRF-3 signaling pathway. *Nat. Immunol.* **4**:491-496.

Graff, J. W., D. N. Mitzel, C. M. Weisend, M. L. Flenniken, and M. E. Hardy. 2002. Interferon regulatory factor 3 is a cellular partner of rotavirus NSP1. *J. Virol.* **76**: 9545-9550.

Graff, J. W., K. Ettayebi, and M. E. Hardy. 2009. Rotavirus NSP1 inhibits NFkappaB activation by inducing proteasome-dependent degradation of β-TrCP: a novel mechanism of IFN antagonism. *PLoS Pathog.* **5**: 21000280.

Hirata, Y., A. H. Broquet, L. Menchen, M. F. Kagnoff. 2007. Activation of innate immune defense mechanisms by signaling through RIG-I/IPS-1 in intestinal epithelial cells. *J. Immunol.* **179**: 5425-5432.

Hoosein, N. M., M. K. McKnight, A. E. Levine, K. M. Mulder, K. E. Childress, D. E. Brattain, and M. G. Brattain. 1989. Differential sensitivity of subclasses of human colon carcinoma cell lines to the growth inhibitory effects of transforming growth factor- a1. *Exp. Cell Res.* **181**: 442-453.

Kaisho, T., and S. Akira. 2005. Toll-like Receptors. *eLS.*

Kato, H., O. Takeuchi, S. Sato, M. Yoneyama, M. Yamamoto, K. Matsui, S. Uematsu, A. Jung, T. Kawai, K. J. Ishii, O. Yamaguchi, K. Otsu, T. Tsujimura, C. Koh, C. Reis e Sousa,

Y. Matsuura, T. Fujita, and S. Akira. 2006. Differential roles of MDA5 and RIG-I helicases in the recognition of RNA viruses. *Nature* **441**: 101-105.

Kaufmann S. H., Desnoyers S., Ottaviano Y., Davidson N. E., Poirier G. G. 1993. Specific Proteolytic Cleavage of Poly(ADP-ribose) Polymerase: An Early Marker of Chemotherapy-induced Apoptosis. *Cancer Res.* **53**: 3976–3985.

Kawai, T., K. Takahashi, S. Sato, C. Coban, H. Kumar, H. Kato, K. J. Ishii, O. Takeuchi, and S. Akira. 2005. IPS-1, an adaptor triggering RIG-1- and Mda5-mediated type I interferon induction. *Nature Immunol.* **6**: 981-988.

Lazebnik, Y. A., S. H. Kaufmann, S. Desnoyers, G. G. Poirier, and W. C. Earnshaw. 1994. Cleavage of poly(ADP-ribose) polymerase by a proteinase with properties like ICE. *Nature* **371**: 346-347.

Le Goffic, R., J. Pothlichet, D. Vitour, T. Fujita, E. Meurs, M. Chignard, and M. Si-Tahar. 2007. Cutting Edge: Influenza A Virus Activates TLR3-Dependent Inflammatory and RIG-I-Dependent Antiviral Responses in Human Lung Epithelial Cells. *J. Immunol.* **178**: 3368-3372.

Medzhitov, R. M. and C. A. Janeway. 2000. Innate immune recognition: Mechanisms and pathways*. Immunol. Rev.* **173**: 89 -97.

Meylan, E., J. Curran, K. Hofmann, D. Moradpour, M. Binder, R. Bartenschlager, and J. Tschopp. 2005. Cardif is an adaptor protein in the RIG-I antiviral pathway and is targeted by hepatitis C virus. *Nature* **437**: 1167-1172.

Mitchell, D. B., and G. W. Both. 1990. Conservation of a potential metal binding motif despite extensive sequence diversity in the rotavirus nonstructural protein NS53. *Virology* **174**: 618-621.

Otte, J. M., E. Cario, and D. K. Podolsky. 2004. Mechanisms of cross hyporesponsiveness to Toll-like receptor bacterial ligands in intestinal epithelial cells. *Gastroenterology* **126**: 1054-1070.

Parashar, U. D., E. G. Hummelman, J. S. Bresee, M. A. Miller, and R. I. Glass. 2003. Global illness and deaths caused by rotavirus disease in children. *Emerg. Infect. Dis.* **9**: 565-572.

Patton, J. T. 1995. Structure and function of the rotavirus RNA-binding proteins. *J. Gen. Virol*. **76**: 2633-2644.

Patton, J. T., Z. Taraporewala, D. Chen, V. Chizhikov, M. Jones, A. Elhelu, M. Collins, K. Kearney, M. Wagner, Y. Hoshino, and V. Gouvea. 2001. Effect of Intragenic

Rearrangement and Changes in the 3' Consensus Sequence on NSP1 Expression and Rotavirus Replication. *J. Virol.* **75**: 2076-2086.

Pott, J., S. Stockinger, N. Torow, A. Smoczek, C. Lindner, G. McInery, F. Backhed, U. Baumann, O. Pabst, A. Bleich, M. W. Hornef. 2012. Age-Dependent TLR3 Expression of the Intestinal Epithelium Contributes to Rotavirus Susceptibility. *PLoS Pathog*. **8**(5): e1002670.

Prasad, B. V. V., G. J. Wang, J. P. M. Clerx, and W. Chiu. 1988. Three-dimensional Structure of Rotavirus. *J. Mol. Biol.* **199**: 269-275.

Qin, L., L. Ren, Z. Zhou, X. Lei, L. Chen, Q. Xue, X. Liu, J. Wang, and T. Hung. 2011. Rotavirus nonstructural protein 1 antagonizes innate immune response by interacting with retinoic acid inducible gene I. *Virology Journal*. **8**: 526.

Ramig, R. F. 2004. Pathogenesis of intestinal and systemic rotavirus infection. *J. Virol*. **78**: 10213-10220.

Rixon, F., P. Taylor, and U. Desselberger. 1984. Rotavirus RNA segments sized by electron microscopy. *J. Gen. Virol.* **65**: 233-239.

Rollo, E. E., K. P. Kumar, N. C. Reich, J. Cohen, J. Angel, H. B. Greenberg, R. Sheth, J. Anderson, B. Oh, S. J. Hempson, E. R. Mackow, and R. D. Shaw. 1999. The epithelial cell response to rotavirus infection. *J. Immunol*. **163**: 4442-4452.

Roseto, A., J. Escaig, E. Delain, J. Cohen, and R. Scherrer. 1979. Structure of rotaviruses as studied by the freeze-drying technique. *Virology* **98**: 471-475.

Rothenfusser, S., N. Goutagny, G. DiPerna, M. Gong, B. G. Monks, A. Schoenemeyer, M. Yamamoto, S. Akira, and K. A. Fitzgerald. 2005. The RNA helicase Lgp2 inhibits TLR-independent sensing of viral replication by retinoic acid-inducible gene-I. *J. Immunol.* **185**: 5260-5268.

Salvesen, G. S. and V. M. Dixit. 1997. Caspases: Intracellular Signaling by Proteolysis. *Cell* **91**: 443-446.

Sato M., N. Hata, M. Asagiri, T. Nakaya, T. Taniguchi, and N. Tanaka. 1998. Positive feedback regulation of type I IFN genes by the IFN-inducible transcription factor IRF-7. *FEBS Lett*. **441**: 106-110b.

Sato M., H. Suemori, N. Hata, M. Asagiri, K. Ogasawara, K. Nakao, T. Nakaya, M. Katsuki, S. Noguchi, N. Tanaka, and T. Taniguchi. 2000. Distinct and Essential Roles of Transcription Factors IRF-3 and IRF-7 Response to Viruses for IFN-α/β Gene Induction. *Immunity* **13**: 539-548.

Saito, T., R. Hirai, Y. M. Loo, D. Owen, C. L. Johnson, S. C. Sinha, S. Akira, T. Fujita, and M. Gale, Jr. 2007. Regulation of innate antiviral defenses through a shared repressor domain in RIG-I and LGP2. *Proc. Natl. Acad. Sci. USA* **104**: 582-587.

Sen, A., A. J. Pruijssers, T. S. Dermody, A. Garcia-Sastre, and H. B. Greenberg. 2011. *J. Virology* **85**: 3717-3732.

Sen, G. C., and S. N. Sarkar. 2005. Transcriptional signaling by double-stranded RNA: role of TLR3. *Cytokine Growth Factor Rev*. **16**: 1-14.

Seth, R. B., L. Sun, C. K. Ea, and Z. J. Chen. 2005. Identification and characterization of MAVS, a mitochondrial antiviral signaling protein that activates NF-kappaB and IRF 3. *Cell* **122**: 669-682.

Sharma, S., B. R. tenOever, N. Grandvaux, G. P. Zhou, R. Lin, J. Hiscott. 2003. Triggering the interferon antiviral response through an IKK-related pathway. *Science* **300**: 1148-1151.

Take, Y., M. Kumano, H. Teraoka, S. Nishimura, and A. Okuyama. 1996. DNA-Dependent Protein Kinase Inhibitor (OK-1035) Suppresses p21 Expression in HCT116 Cells Containing Wild-Type p53 Induced by Adriamycin. *Biochem. Biophys. Res. Commun*. **221**: 207-212.

Takeda, K., T. Kaisho, and S. Akira. 2003. Toll-like receptors. *Annu. Rev. Immunol.* **21**:335-376.

Taniguchi, K., K. Kojima, and S. Urasawa. 1996. Nondefective rotavirus mutants with an NSP1 gene which has a deletion of 500 nucleotides, including a cysteine-rich zinc finger motif-encoding region (nucleotides 156 to 248), or which has a nonsense codon at nucleotides 153 to 155. *J. Virol.* **70**: 4125-4130.

Taniguchi, T., K. Ogasawara, A. Takaoka, and N. Tanaka. 2001. IRF Family of Transcription Factors as Regulators of Host Defense. *Annu Rev. Immunol*. **19**: 623-655.

Taniguchi, T. and A. Takaoka. 2002. The interferon-α/β system in antiviral responses: a multimodal machinery of gene regulation by the IRF family of transcription factors. *Current Opinion in Immunology*. **14**: 111-116.

Taura, M., A. Eguma, M. A. Suico, T. Shuto, T. Koga, K. Komatsu, T. Komune, T. Sato, H. Saya, J. Li, and H. Kai. 2008. p53 regulates Toll-like receptor 3 expression and function in human epithelial cell lines. *Mol. Cell. Bio.* **28**: 6557-6567.

Wilhelmi, I., E. Roman, and A. Sanchez-Fauquier. 2003. Viruses causing gastroenteritis. *Clin. Microbiol. Infect*. **9**: 247-262.

Wolfe, N. D., C. P. Dunavan, and J. Diamond. 2007. Origins of major human infectious diseases. *Nature* **447**: 279-283.

Xu, L. G., Y. Y. Wang, K. J. Han, L. Y. Li, Z. Zhai, and H. B. Shu. 2005. VISA is an adaptor protein required for virus-triggered IFN-β signaling. *Mol. Cell* **19**: 727-740.

Yamamoto, M., S. Sato, H. Hemmi, K. Hoshino, T. Kaisho, H. Sanjo, O. Takeuchi, M. Sugiyama, M. Okabe, K. Takeda, and S. Akira. 2003. Role of Adaptor TRIF in the MyD88-Independent Toll-like Receptor Signaling Pathway. *Science*. **301**: 640-642.

Yoneyama, M., W. Suhara, Y. Fukuhara, M. Fukuda, E. Nishida, T. Fujita. 1998. Direct triggering of the type I interferon system by virus infection: cativation of a transcription factor complex containing IRF-3 and CBP/p300. *EMBO J.* **17**: 1087-1095.

Yoneyama, M., M. Kikuchi, T. Natsukawa, N. Shinobu, T. Imaizumi, M. Miyagishi, K. Taira, S. Akira, and T. Fujita. 2004. The RNA helicase RIG-I has an essential function in double-stranded RNA-induced innate antiviral responses. *Nature Immunol*. **7**: 730-737.

Yoneyama, M., M. Kikuchi, K. Matsumoto, T. Imaizumi, M. Miyagishi, K. Taira, E. Foy, Y. M. Loo, M. Gale Jr., S. Akira, S. Yonehara, A. Kato, and T. Fujita. 2005. Shared and unique functions of the DExD/H-box helicases RIG-I, MDA5, and LGP2 in antiviral innate immunity. *J. Immunol.* **175**: 2851-2858.

Zhou, R., H. Wei, R. Sun, and Z. Tian. 2007. Recognition of Double-Stranded RNA by TLR3 Induces Severe Small Intestinal Injury in Mice. *J. Immunol*. **176**: 4548-4556.